

論文 / 著書情報  
Article / Book Information

Title	Magnetic anisotropy of [Co <sub>2</sub> MnSi/Pd] <sub>n</sub> superlattice films prepared on MgO(001), (110), and (111) substrates
Authors	N. Matsushita,Y. Takamura,Y. Fujino,Y. Sonobe,S. Nakagawa
Citation	Appl. Phys. Lett., Vol. 106, No. 6,
Pub. date	2015, 2
URL	<a href="http://scitation.aip.org/content/aip/journal/apl">http://scitation.aip.org/content/aip/journal/apl</a>
Copyright	Copyright (c) 2015 American Institute of Physics

## Magnetic anisotropy of [Co<sub>2</sub>MnSi/Pd]<sub>n</sub> superlattice films prepared on MgO(001), (110), and (111) substrates

Naoki Matsushita, Yota Takamura, Yorinobu Fujino, Yoshiaki Sonobe, and Shigeki Nakagawa

Citation: [Applied Physics Letters](#) **106**, 062403 (2015); doi: 10.1063/1.4907892

View online: <http://dx.doi.org/10.1063/1.4907892>

View Table of Contents: <http://scitation.aip.org/content/aip/journal/apl/106/6?ver=pdfcov>

Published by the [AIP Publishing](#)

---

### Articles you may be interested in

[Highly \(001\) oriented L10-CoPt/TiN multilayer films on glass substrates with perpendicular magnetic anisotropy](#)  
J. Vac. Sci. Technol. A **33**, 021512 (2015); 10.1116/1.4905847

[CoTaZr/Pd multilayer with perpendicular magnetic anisotropy](#)  
APL Mat. **1**, 022104 (2013); 10.1063/1.4818004

[Fabrication of perpendicularly magnetized magnetic tunnel junctions with L10-CoPt / Co2MnSi hybrid electrode](#)  
J. Appl. Phys. **107**, 09C714 (2010); 10.1063/1.3358239

[MgO barrier-perpendicular magnetic tunnel junctions with CoFe/Pd multilayers and ferromagnetic insertion layers](#)  
Appl. Phys. Lett. **95**, 232516 (2009); 10.1063/1.3265740

[The structure of sputter-deposited Co2MnSi thin films deposited on GaAs \(001\)](#)  
J. Appl. Phys. **101**, 023915 (2007); 10.1063/1.2424529

---



# Magnetic anisotropy of $[\text{Co}_2\text{MnSi}/\text{Pd}]_n$ superlattice films prepared on $\text{MgO}(001)$ , $(110)$ , and $(111)$ substrates

Naoki Matsushita,<sup>1</sup> Yota Takamura,<sup>1</sup> Yoronobu Fujino,<sup>1</sup> Yoshiaki Sonobe,<sup>2</sup> and Shigeki Nakagawa<sup>1,a)</sup>

<sup>1</sup>Department of Physical Electronics, Tokyo Institute of Technology, 2-12-1 Ookayama, Meguro-ku, Tokyo 152-8552, Japan

<sup>2</sup>Samsung R&D Institute Japan-Yokohama, 2-7, Sugasawa-cho, Tsurumi-ku, Yokohama-shi, Kanagawa-ken 230-0027, Japan

(Received 10 December 2014; accepted 29 January 2015; published online 9 February 2015)

Superlattice films with full-Heusler  $\text{Co}_2\text{MnSi}$  (CMS) alloy and Pd layers prepared on Pd-buffered  $\text{MgO}(001)$ ,  $(110)$ , and  $(111)$  substrates were investigated. Crystal orientation and epitaxial relationship of Pd and CMS layers were analyzed from x-ray diffraction, pole figure measurements, and transmission electron microscope observation. Formation of the  $L2_1$ -ordered structure in the CMS layers was confirmed by observation of CMS(111) diffraction. Perpendicular magnetic anisotropy (PMA) was obtained in the  $[\text{CMS}(0.6\text{ nm})/\text{Pd}(2\text{ nm})]_6$  superlattice film formed using  $\text{MgO}(111)$  substrates although other superlattice films prepared using  $\text{MgO}(001)$  and  $(110)$  substrates showed in-plane and isotropic magnetic anisotropy, respectively. The perpendicular magnetic anisotropy energy constant  $K$  for the superlattice films prepared using  $\text{MgO}(111)$  substrate was estimated to be  $2.3\text{ Mergs/cm}^3$ , and an interfacial anisotropy constant  $K_i$  per one CMS-Pd interface in the superlattice films was estimated to be  $0.16\text{ ergs/cm}^2$ .  $K_i$  in superlattice films with various crystal orientations showed positive values, indicating that Pd/CMS interfaces had an ability to induce PMA regardless of their crystal orientation. © 2015 AIP Publishing LLC.

<http://dx.doi.org/10.1063/1.4907892>

Highly spin-polarized ferromagnetic materials with perpendicular magnetic anisotropy (PMA) are very attractive for future spintronics device applications, such as perpendicular magnetic tunnel junctions (p-MTJs)<sup>1–3</sup> and magnetic domain-motion memory devices,<sup>4–6</sup> since they can realize extremely high tunnel magnetoresistance (TMR), low spin transfer torque currents for magnetization switching and for magnetic domain wall motion. One of the highest spin polarized materials are half-metallic ferromagnets (HMFs)<sup>7</sup> with the perfect spin polarization of 100%. Most of Co-based full-Heusler alloys such as  $\text{Co}_2\text{MnSi}$  (CMS),<sup>8</sup>  $\text{Co}_2\text{FeSi}$ ,<sup>9</sup> and  $\text{Co}_2\text{FeSi}_{1-x}\text{Al}_x$ <sup>10</sup> are theoretically predicted as HMFs with high Curie temperatures. In particular, half-metallicity of CMS was experimentally confirmed by extremely high TMR ratios up to 1995% at 4.2 K and 354% at 290 K observed in in-plane MTJs.<sup>11</sup> On the other hand, these half-metallic full-Heusler alloys do not have intrinsic PMA, since they have a highly symmetric cubical crystal structure. Addition of PMA to several ferromagnetic materials without intrinsic PMA was attained by MgO-induced interfacial anisotropy in Fe-based ferromagnetic films, e.g., Fe,<sup>12</sup>  $\text{CoFeB}$ ,<sup>3</sup> and  $\text{Co}_2\text{FeSi}$ .<sup>13</sup> Since the key factor in this technique is considered to be the hybridization of orbital of the Fe-O bonding,<sup>12,14</sup> this technique cannot be applied to CMS. Another way to add PMA is to form superlattice films that are a multi-stacking structure with alternating layers of different materials. For instance, superlattice films composed of Co and Pt or Pd layers formed on  $\text{MgO}(111)$  substrates are well known to show PMA,<sup>15</sup> which were used as the pinned layers in p-MTJ. Additionally, non-half-metallic full-Heusler  $\text{Co}_2\text{FeAl}$  alloys have been

reported to show PMA by forming superlattice films with Pt on  $\text{MgO}(001)$  substrates.<sup>16</sup> In this paper, we fabricated full-Heusler CMS alloy films and superlattice films composed of CMS and Pd (hereafter, this structure is referred to as  $[\text{CMS}/\text{Pd}]_n$ ) using MgO substrates with various crystal orientations of  $(001)$ ,  $(110)$ , and  $(111)$ . We demonstrated that superlattice films formed using  $\text{MgO}(111)$  substrates showed PMA. A relationship between crystal orientation and magnetic property of the  $[\text{CMS}/\text{Pd}]_n$  superlattice films was investigated.

All the specimen films were prepared using our developed DC Facing Targets Sputtering system<sup>17</sup> with a base pressure below  $9.0 \times 10^{-5}\text{ Pa}$ . The substrate temperature during sputtering was  $300^\circ\text{C}$ . Kr gas was used for the sputtering. Gas pressures for CMS, Pd, and Ta sputtering were 0.52, 0.13, and 0.13 Pa, respectively. Deposition rates of these layers were 0.060, 0.027, and 0.077 nm/s, respectively. Crystal structures of the samples were evaluated by out-of-plane x-ray diffraction (XRD) measurements with a Cu-K $\alpha$  source and transmission electron microscope (TEM) observation. Magnetic properties were evaluated by vibrating sample magnetometer (VSM) measurement, in which the contribution from the MgO substrate was subtracted. PMA energy constant  $K$  was estimated from the difference of magnetization energy between in-plane and out-of-plane  $M$ - $H$  curves.

First, crystallographic features of Pd/CMS bilayers sputtered on MgO substrates with various crystal orientations were evaluated by XRD. The sample structures were  $\text{MgO}$ -substrates/Pd (20)/CMS (60)/Ta-capping layers (the numbers in parentheses are the film thickness in nanometer), where crystal orientations of the MgO substrates were  $(001)$ ,  $(110)$ , and  $(111)$ . Figure 1 shows XRD diagrams of the Pd/CMS

<sup>a)</sup>Electronic mail: nakagawa@pe.titech.ac.jp

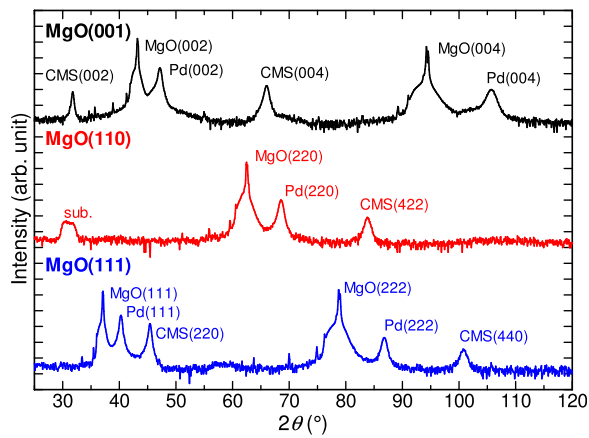


FIG. 1. XRD diagrams of Pd/CMS bilayers formed on MgO(001), (110), and (111) substrates.

bilayer samples. When an MgO(001) substrate was used, both Pd and CMS layers showed (001) orientation. When an MgO(110) substrate was used, only Pd(220) and CMS(422) peaks appeared, indicating that the orientations of Pd and CMS layers were (110) and (211), respectively. Note that a peak observed around  $2\theta = 32^\circ$  (that is, near the position of CMS(200) diffraction peak) was a spurious signal from the MgO(110) substrate. When an MgO(111) substrate was used, the Pd and CMS layers showed (111) and (220) orientations, respectively.

In-plane epitaxial relationship among the MgO substrate, Pd, and CMS layers of the samples was analyzed by x-ray pole figure scans. Figures 2(a)–2(c), 2(d)–2(f), and 2(g)–2(i) show pole figures for the Pd/CMS bilayer films prepared using MgO(001), (110), and (111) substrates, respectively, in which top, middle, and bottom panels show pole figures for MgO, Pd, and CMS diffraction, respectively. For the Pd/CMS films

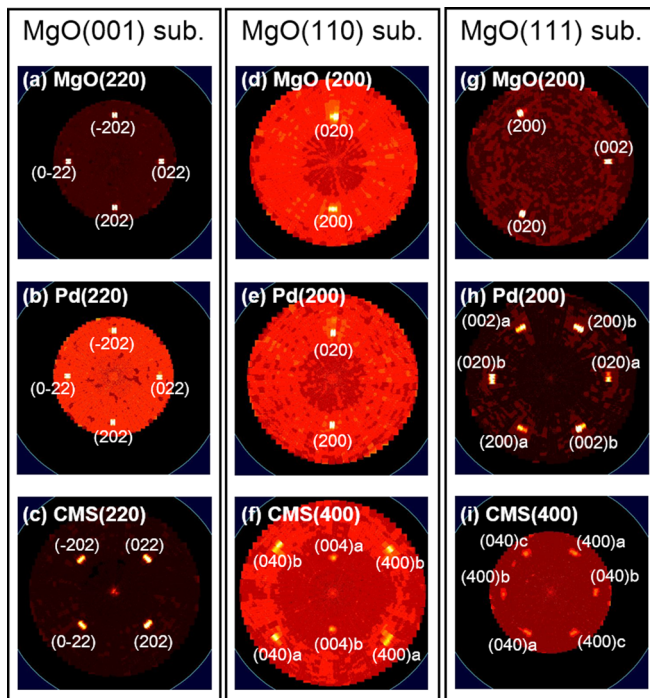


FIG. 2. X-ray pole figures of MgO, Pd and CMS for the Pd/CMS bilayer samples prepared using MgO(001), (110), and (111) substrates.

formed on the MgO(001) substrate, all the peaks showed four-fold symmetry with respect to the in-plane rotation angle,  $\varphi$ . Diffraction peaks from Pd were observed at same angles of diffraction of MgO substrates, and those from CMS were shifted by  $45^\circ$  with respect to each of MgO and Pd diffraction peaks. This crystallographic relationship can be expressed as  $\text{MgO}(001) [100] \parallel \text{Pd}(001) [100] \parallel \text{CMS}(001) [110]$ . This relationship can be explained that the lattice constant of CMS is almost same as square root of 2 times that of Pd. For a case of the MgO(110) substrate, Pd(200) peaks showed twofold symmetry at tilt angle  $\psi = 45.0^\circ$  as well as MgO(200), indicating that the single crystalline Pd layer was grown. On the other hand, CMS(400) diffraction peaks showed two components as shown in Fig. 2(f). This indicated that the CMS layer had a twinned crystal structure rotated by  $180^\circ$  each other. For the sample on the MgO(111) substrate, the Pd and CMS layers showed two and three orientation components in the plane, respectively.

The  $L_{21}$ -ordered structure of full-Heusler CMS alloys is very important to obtain their half-metallic nature, since the half-metallicity cannot be obtained for the other disorder structures, such as A2 and B2.<sup>18</sup> Ordered crystal structures of full-Heusler alloys can be distinguished by superlattice diffraction, i.e., when the  $L_{21}$  structure was formed, (111) and (200) superlattice diffraction peaks appear.<sup>19,20</sup> CMS(111) diffraction peaks for all the CMS films were measured with appropriate tilt and in-plane angles since the CMS thin films were oriented. Figure 3 shows CMS(111) diffraction patterns for all the samples. Detailed goniometer angles for each sample were also shown in Fig. 3. From this analysis, formation of the  $L_{21}$  structure was confirmed for all the CMS layers formed using MgO(001), (110), and (111) substrates.

Magnetic properties of the Pd/CMS bilayer samples were evaluated. All the samples showed in-plane magnetic anisotropy. The saturation magnetization  $M_s$  of the Pd/CMS bilayers formed on MgO(001), (110), and (111) substrates was 706, 695, and 744 emu/cm<sup>3</sup>, respectively. These values were slightly smaller than a bulk value.<sup>21</sup> This decrement may be caused by degradation of crystallinity.

[CMS/Pd]<sub>n</sub> superlattice films were fabricated using the same sputtering condition as the above-described Pd/CMS bilayers. The sample structures were MgO-substrates/Pd(20)/[CMS( $t_{\text{CMS}}$ )/Pd(2)]<sub>6</sub>/Ta-capping layers, where the crystal

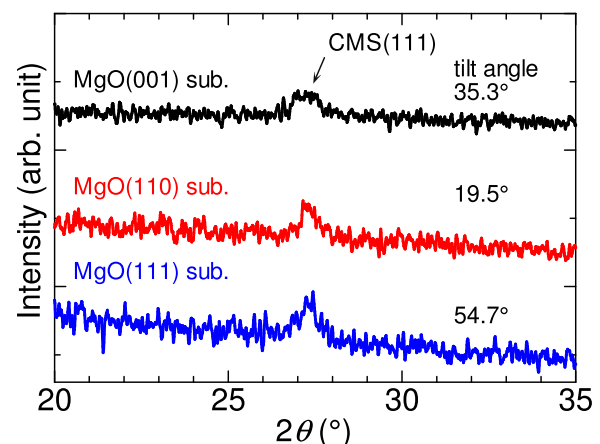


FIG. 3. CMS (111) diffraction peaks for CMS films prepared on Pd-buffered MgO(001), (110), and (111) substrates.



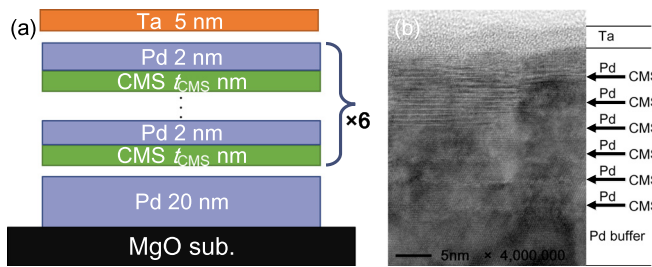


FIG. 4. (a) Schematic structure of  $[\text{CMS}/\text{Pd}]_6$  superlattice films using MgO(001), (110), and (111) substrates. (b) Cross section TEM image for superlattice films formed using MgO(111) substrate.

orientations of the MgO substrates were (001), (110), and (111). The schematic superlattice film structure was shown in Fig. 4(a). The number of the CMS/Pd bilayers in superlattice films was fixed to 6. In XRD diagrams, the satellite peaks were confirmed for all the superlattice films, which suggest that the periodic layered structures were formed. Crystallization in the superlattice region was confirmed by cross section transmission electron microscope observation (Fig. 4(b)), although continuous layer growth of CMS was not clarified from this TEM image.

Figures 5(a)–5(c) show magnetization characteristics of the  $[\text{CMS}/\text{Pd}]_6$  superlattice films with  $t_{\text{CMS}} = 0.6$  nm formed using MgO(001), (110), and (111) substrates, respectively. Red and blue curves in Fig. 5 show  $M$ - $H$  loops for in-plane and out-of-plane magnetic fields, respectively. The longitudinal axes were magnetization divided by  $M_s$  of each loop. The  $[\text{CMS}/\text{Pd}]_6$  superlattice films fabricated using the MgO(001) and (110) substrates showed in-plane and isotropic magnetic anisotropy, respectively. On the other hand,  $M$ - $H$  loops for the superlattice film fabricated using the MgO(111) substrate clearly showed PMA with a good squareness ratio as shown in Fig. 5(c).  $M_s$  for the superlattice films formed using the MgO(111) substrate was  $971 \text{ emu}/\text{cm}^3$ . The increment of  $M_s$  of the superlattice film was due to the influence of polarization at CMS/Pd interfaces. The coercivity of the superlattice film was 259 Oe. The PMA energy constant  $K$  of the superlattice film was estimated to be  $2.3 \text{ Mergs}/\text{cm}^3$ . This  $K$  value was consistent with that of a  $[\text{Co}_2\text{FeAl}/\text{Pt}]_n$  superlattice film.<sup>16</sup>

Magnetic anisotropy at the interfaces in superlattice films was investigated by changing the CMS layer thickness  $t_{\text{CMS}}$ . Figure 6 shows the product of  $K$  and  $t_{\text{CMS}}$  as a function of  $t_{\text{CMS}}$ .  $K \cdot t_{\text{CMS}}$  linearly decreased with increasing  $t_{\text{CMS}}$ . Negative  $K \cdot t_{\text{CMS}}$  values mean in-plane magnetic anisotropy. The intercept of the vertical axis corresponds to the CMS-Pd interfacial magnetic anisotropy, which was positive for superlattice films formed using MgO with all the crystal

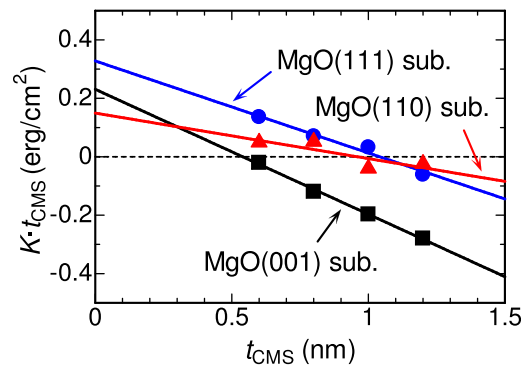


FIG. 6. The product of magnetic anisotropy constant  $K$  and CMS layer thickness  $t_{\text{CMS}}$  as a function of  $t_{\text{CMS}}$ .

orientations. This indicated that magnetic anisotropy of the CMS/Pd interface was perpendicular regardless of its crystal orientation. An interfacial anisotropy  $K_i$  per one CMS-Pd interface was quantitatively estimated by fitting using a relation of  $K \cdot t_{\text{CMS}} = K_V \cdot t_{\text{CMS}} + 2K_i$ , where  $K_V$  is a magnetic anisotropy energy of CMS.  $K_i$  for superlattice films formed using MgO(001), (110), and (111) substrates was 0.12, 0.08, and  $0.16 \text{ ergs}/\text{cm}^2$ , respectively. The largest  $K_i$  was observed for the superlattice films formed on MgO(111) substrate.  $K_V$  for superlattice films formed using MgO(001), (110), and (111) substrates was  $-4.3$ ,  $-1.6$ , and  $-3.1 \text{ Mergs}/\text{cm}^3$ , respectively. The largest  $K_V$  was observed for the superlattice films formed using MgO(110) substrate. This difference was considered to be crystal magnetic anisotropy.

In summary, superlattice films with full-Heusler CMS alloy and Pd layers prepared on Pd-buffered MgO(001), (110), and (111) substrates were investigated. Crystal orientation and epitaxial relationship of Pd and CMS layers were analyzed using x-ray diffraction, pole figure measurements, and transmission electron microscope observation. Formation of the  $L2_1$ -ordered structure in the CMS layers was confirmed by observation of CMS(111) diffraction. PMA was obtained in the  $[\text{CMS} (0.6 \text{ nm})/\text{Pd} (2 \text{ nm})]_6$  superlattice film formed using MgO(111) substrates although other superlattice films formed using MgO(001) and (110) substrates showed in-plane and isotropic magnetic anisotropy, respectively. The PMA energy constant  $K$  for the superlattice films formed using the MgO(111) substrate was estimated to be  $2.3 \text{ Mergs}/\text{cm}^3$ , and an interfacial anisotropy constant  $K_i$  per one CMS-Pd interface in the superlattice was estimated to be  $0.16 \text{ ergs}/\text{cm}^2$ .  $K_i$  in superlattice films with various crystal orientations showed positive values, indicating that Pd/CMS interfaces had an ability to induce PMA regardless of their crystal orientation.

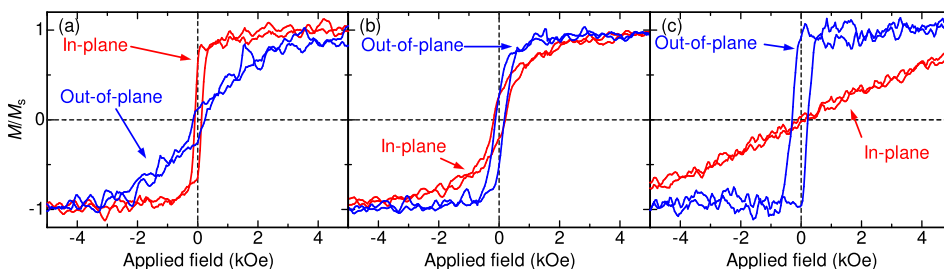


FIG. 5. Magnetic properties of  $[\text{CMS}(0.6 \text{ nm})/\text{Pd}(2 \text{ nm})]_6$  superlattice films formed on Pd-buffered MgO(001), (110), and (111) substrates.

A part of this work was supported by JSPS KAKENHI Grant No. 25889021. A part of x-ray diffraction measurements was performed at the Center for Advanced Materials Analysis (CAMA), Tokyo Institute of Technology, Japan.

- <sup>1</sup>S. Mangin, D. Ravelosona, J. A. Katine, M. J. Carey, B. D. Terris, and E. E. Fullerton, *Nat. Mater.* **5**, 210 (2006).
- <sup>2</sup>H. Ohmori, T. Hatori, and S. Nakagawa, *J. Appl. Phys.* **103**, 07A911 (2008).
- <sup>3</sup>S. Ikeda, K. Miura, H. Yamamoto, K. Mizunuma, H. D. Gan, M. Endo, S. Kanai, J. Hayakawa, F. Matsukura, and H. Ohno, *Nat. Mater.* **9**, 721 (2010).
- <sup>4</sup>S. S. P. Parkin, M. Hayashi, and L. Thomas, *Science* **320**, 190 (2008).
- <sup>5</sup>H. Tanigawa, K. Kondou, T. Koyama, K. Nakano, S. Kasai, N. Ohshima, S. Fukami, N. Ishiwata, and T. Ono, *Appl. Phys. Express* **1**, 11301 (2008).
- <sup>6</sup>M. Okuda, Y. Miyamoto, M. Kishida, and N. Hayashi, *IEEE Trans. Magn.* **47**, 2525 (2011).
- <sup>7</sup>R. A. de Groot, F. M. Mueller, P. G. van Engen, and K. H. J. Buschow, *Phys. Rev. Lett.* **50**, 2024 (1983).
- <sup>8</sup>T. Ishikawa, T. Marukame, H. Kijima, K. I. Matsuda, T. Uemura, M. Arita, and M. Yamamoto, *Appl. Phys. Lett.* **89**, 192505 (2006).
- <sup>9</sup>Y. Takamura, R. Nakane, H. Munekata, and S. Sugahara, *J. Appl. Phys.* **103**, 07D719 (2008).
- <sup>10</sup>B. Balke, S. Wurmehl, G. H. Fecher, C. Felser, and J. Kübler, *Sci. Technol. Adv. Mater.* **9**, 014102 (2008).
- <sup>11</sup>H. Liu, Y. Honda, T. Taira, K. Matsuda, M. Arita, T. Uemura, and M. Yamamoto, *Appl. Phys. Lett.* **101**, 132418 (2012).
- <sup>12</sup>R. Shimabukuro, K. Nakamura, T. Akiyama, and T. Ito, *Physica E* **42**, 1014 (2010).
- <sup>13</sup>Y. Takamura, T. Suzuki, Y. Fujino, and S. Nakagawa, *J. Appl. Phys.* **115**, 17C732 (2014).
- <sup>14</sup>J. Okabayashi, J. W. Koo, H. Sukegawa, S. Mitani, Y. Takagi, and T. Yokoyama, *Appl. Phys. Lett.* **105**, 122408 (2014).
- <sup>15</sup>H. Ohmori and A. Maesaka, *J. Magn. Soc. Jpn.* **26**, 224 (2002).
- <sup>16</sup>W. Wang, H. Sukegawa, and K. Inomata, *Appl. Phys. Express* **3**, 093002 (2010).
- <sup>17</sup>M. Naoe, S. Yamanaka, and Y. Hoshi, *IEEE Trans. Magn.* **16**, 646 (1980).
- <sup>18</sup>Y. Miura, K. Nagao, and M. Shirai, *Phys. Rev. B* **69**, 144413 (2004).
- <sup>19</sup>P. J. Webster and K. R. A. Ziebeck, *J. Phys. Chem. Solids* **34**, 1647 (1973).
- <sup>20</sup>Y. Takamura, R. Nakane, and S. Sugahara, *J. Appl. Phys.* **105**, 07B109 (2009).
- <sup>21</sup>S. Kammerer, A. Thomas, A. Hutten, and G. Reiss, *Appl. Phys. Lett.* **85**, 79 (2004).